International Journal of New Technology and Research (IJNTR)
ISSN:2454-4116, Volume-4, Issue-4, April 2018 Pages 91-96

Interleaved Boost Converter with Coupled Inductor – Theory and Application

Miriam Jarabicova, Slavomir Kascak, Michal Prazenica

***Abstract*—This paper describe the analysis of interleaved boost DC-DC converter with a coupled inductor on the same magnetic core. The advantage of the coupled inductor over the non-coupled case is investigated. The current ripple equations as an input current for the boost operation mode and the ripple current in individual phase of the interleaved converter using coupled inductor are explained analytically, supported by simulation and experimental results. The novelty of the paper is an investigation of current ripples of interleaved boost converter operated over 50 % of duty ratio and utilization of the converter in the application of electric drive vehicle.**

***Index Terms*— Interleaved boost converter, coupled inductors, coupling coefficient, bidirectional converter.**

I. Introduction

Nowadays, the interleaved topologies are widely used due to their advantageous properties such as lowered current ripple and volume reduction [1]- [9].

For the higher power applications, there are more possibilities how to perform higher power density regarding the efficiency of the converter. The first choice is to utilize of the paralleling of the power switches, shown in Fig. 1. This converter includes only one inductor and parallel connected two half-bridge legs. This is done for reasons of obtaining higher current ratings, thermal improvements, and sometimes for redundancy. If losses are not equally shared, the thermal differences between the devices will lead to other problems and possible failure of the transistors. Therefore, the thermal coefficient of the collector-emitter voltage $V_{CE(SAT)}$ is an important parameter when paralleling IGBTs. It must be a positive to allow current sharing. On the other hand, the higher positive thermal coefficient the higher losses arise because at high temperature the $V_{CE(SAT)}$ is increased.

The second option how to share the current is to use the interleaved topology, Fig. 2 [10] – [13]. The same problem as in the previous topology with current sharing is eliminated because the current is divided between two parallel boost converters. The benefits are in improved power density, the interleaved effect reduces the total input and output current ripple, so this means the smaller input and output filters (bulk capacitor), better distribution of power with lower current stress for semiconductor devices [3] – [8].

In the high current application, there are used the interleaved topologies even with the coupled inductors. The advantage of the coupled inductor is in lowered current ripple direct on the inductors not only in the output or input current of the converters. The interleaved buck converter with a coupled inductor is used in VRM application where voltage about 1V and current of hundreds of amps are applied. On the other side, utilization of coupled inductor in higher voltage application does not have any limitation as is seen in PFC application [14]- [18]. Therefore, the advantageous features of the coupled inductor will be analyzed for the converter, which serves for boosting voltage from ultracapacitor/battery to DC bus for driving traction motor.

The analysis includes investigation of current ripple – on the input of the converter and change of the inductor current ripple in case of the coupled inductor in comparison with the non-coupled case.

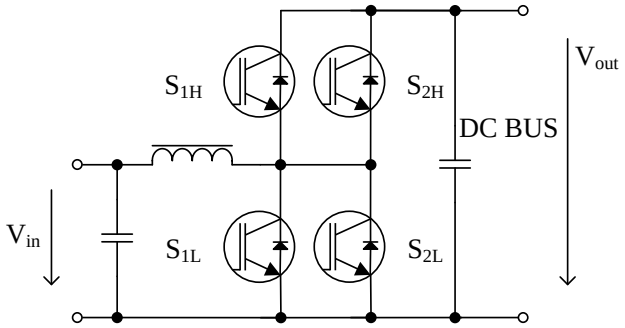

Fig. 1:Boost DC/DC converter for higher power application

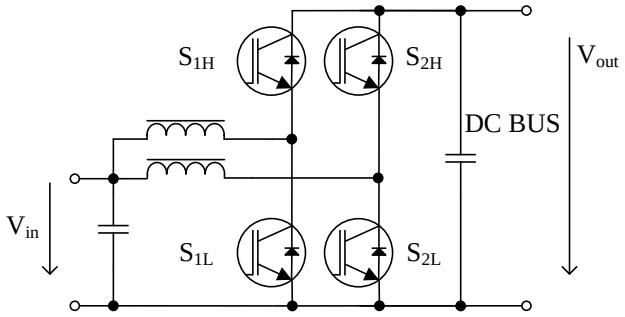

Fig. 2:Interleaved boost DC/DC converter for battery/ultracapacitor application

II. Reduction of Current Ripple

The intention of the current ripple reduction in case of battery application is to prolong the battery service life because is sensitive to high dynamic current stress. Therefore,

Slavomir Kascak, Department OF Mechatronics and Electronics, Faculty of Electrical Engineering, University of Zilina, Univerzitna 1, Zilina, Slovakia
Michal Prazenica, Department OF Mechatronics and Electronics, Faculty of Electrical Engineering, University of Zilina, Univerzitna 1, Zilina, Slovakia
Miriam Jarabicova, Department OF Mechatronics and Electronics, Faculty of Electrical Engineering, University of Zilina, Univerzitna 1, Zilina, Slovakia

the boost interleaved topology with reduced input current ripple is proposed to solve this issue. The input of the converter shown in Fig. 2 is connected to the battery/ultracapacitor pack and output to the DC BUS of the three-phase inverter.

This section is divided into two parts. Firstly, an impact of the non-coupled inductor on boost topology is investigated. Then, in some following subheads, the advantage of coupled inductor is analyzed with emphasis to the reduced inductor current ripple.

In the two-phase interleaved converter, the four different operating modes occur as shown in Fig. 3. The first interval begins when the switch S_{1L} and S_{2H} are closed, the second interval when S_{1H} and S_{2H} are on. In the third interval, S_{2L} and S_{1H} are turn on. It means that the curve of the current i_L2 in the second phase is same as the current i_{L1} in the first interval, but phase-shifted by 180°. Therefore, the ripple of currents in the third interval is same as in first one (exchange of current i_{L2} with i_{L1} and vice versa). From the Fig. 3 is seen that ripples ΔI_{L1} and ΔI_{L2} are the same. But, the input current ripple is dependent on ΔI_{L1} and ΔI_{L2pp}, not ΔI_{L2}. Then, an appropriate equation for inductor current ripples in a first interval can be obtained, (1) and (2).

$$\Delta I_{L1} = \frac{V_{out}}{L}(1-D)DT_S \tag{1}$$

$$\Delta I_{L2\,pp} = -\frac{V_{in}}{L}(D)DT_S \tag{2}$$

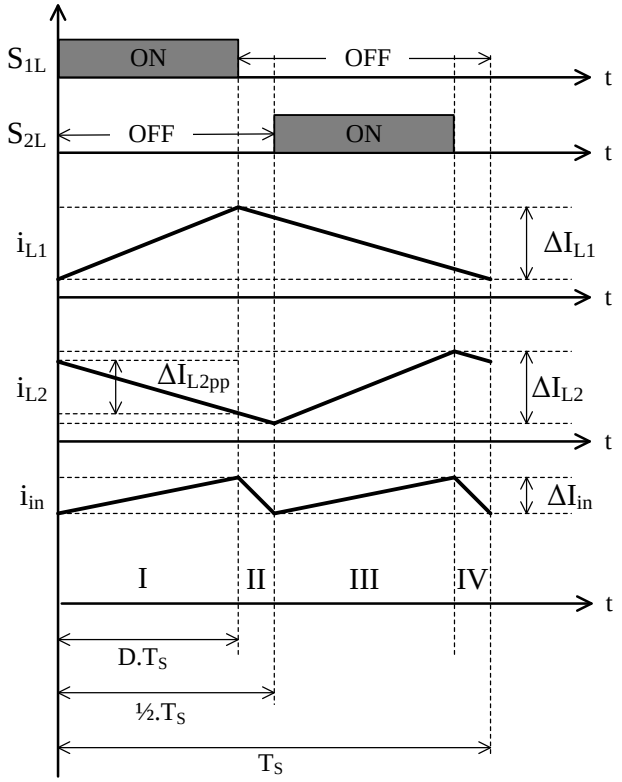

Fig. 3:Current ripples of interleaved non-coupled boost converter

Then, by summing (1) and (2) the equation for input current ripple reduction is:

$$\Delta I_{in} = \Delta I_{L1} + \Delta I_{L2\,pp} = \frac{V_{out}}{L}(1-2D)DT_S \tag{3}$$

Using the same procedure, it can be achieved the input current ripple calculation for all intervals. On the other hand, in case of the steady state, it is not necessary because the current ripple in all interval is the same.

A. *Interleaved Coupled Boost Converter*

A simplified schematic for a coupled boost converter is depicted in Fig. 4. The two-phase coupled boost converter is divided into four intervals same as in the non-coupled case, Fig. 5.

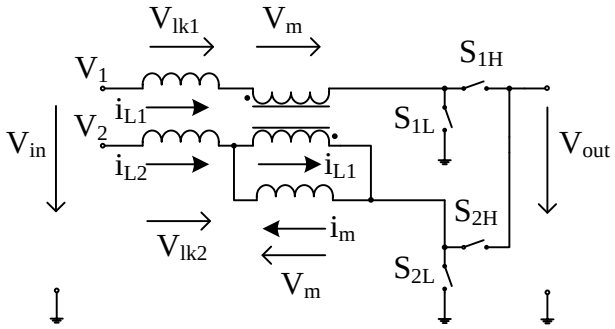

Fig. 4:A simplified schematic of dual interleaved boost converter using coupled inductor

According to Kirchhoff's law the following equation for two-phase coupled buck converter in the first interval can be written (4) - (8):

$$i_{in} = i_{L1} + i_{L2} \tag{4}$$

$$i_m = i_{L1} - i_{L2} \tag{5}$$

$$V_{lk1} = V_{in} - V_m \tag{6}$$

$$V_{lk2} = V_{in} - V_{out} + V_m \tag{7}$$

$$V_m = \frac{L_m}{L_{lk} + 2L_m} V_{out} \tag{8}$$

Using the mathematical apparatus, the following equations refer to the first interval of operation are given, (9) – (11):

$$\Delta I_{L1} = \frac{V_{out}}{L_{lk}}\left(1 - D - \frac{L_m}{L_{lk} + 2L_m}\right)DT_S \tag{9}$$

$$\Delta I_{L2\_I} = \frac{V_{out}}{L_{lk}}\left(\frac{L_m}{L_{lk} + 2L_m} - D\right)DT_S \tag{10}$$

$$\Delta I_{in} = \Delta I_{L1} + \Delta I_{L2\_I} = \frac{V_{out}}{L_{lk}}(1-2D)DT_S \tag{11}$$

These equations also apply for the third interval with the difference that ΔI_{L1} is ΔI_{L2} and vice versa. Using Kirchhoff's laws, the equations for the second interval are as follows, (12) - (14).

$$V_{lk1} = V_{in} - V_{out} - V_m \tag{12}$$

$$V_{lk2} = V_{in} - V_{out} + V_m \tag{13}$$

$$V_m = 0 \tag{14}$$

Using the same procedure as in interval I and III we can obtain current ripples in interval II and IV. The given equations are as follows:

$$\Delta I_{L1\_II} = \Delta I_{L2\_II} = -\frac{V_{out}}{L_{lk}}(0.5-D)DT_S \tag{15}$$

$$\Delta I_{in} = \Delta I_{L1\_II} + \Delta I_{L2\_II} = -\frac{V_{out}}{L_{lk}}(1-2D)DT_S \tag{16}$$

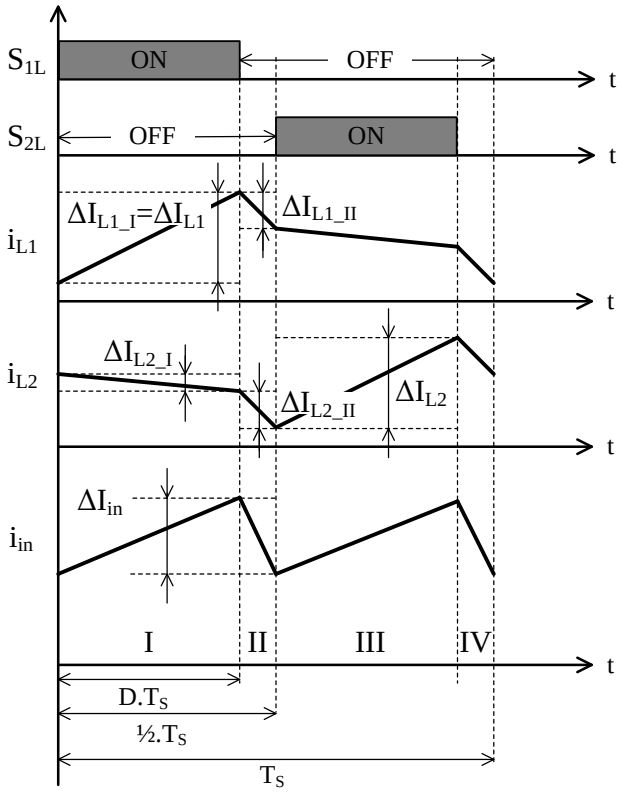

Fig. 5:Current ripples of interleaved coupled boost converter for D < 0.5

For the second and fourth interval of operation, the ripple is same for both phase currents. If we want to determine the total inductor current ripple we must sum the ripple currents in interval II, III and IV or calculate the ripple in interval I. For the ripple current in the second phase we can apply the same approach with the difference that we must calculate the ripple in III interval. On the other hand, the input current ripple is the sum of inductor current ripples corresponding to each time interval.

The operation of boost interleaved converter with duty ratio over 0.5 is shown in a Fig. 6. From this figure is seen that upper switches of the converter can be switched on at once (interval I and III). It means that in this interval the magnetizing voltage V_m equals zero. Analytically, it is stated in some following equations (17) – (22).

$$V_{lk1} = V_{in} - V_m \tag{17}$$

$$V_{lk2} = V_{in} + V_m \tag{18}$$

$$V_m = 0 \tag{19}$$

$$d = D - 0.5 \tag{20}$$

$$\Delta I_{L1\_I} = \Delta I_{L2\_I} = \frac{V_{out}}{L_{lk}}(1-D)(D-0.5)T_S \tag{21}$$

$$\Delta I_{in} = \Delta I_{L1\_I} + \Delta I_{L2\_I} = \frac{V_{out}}{L_{lk}}(2-2D)(D-0.5)T_S \tag{22}$$

Similarly, for the II and IV interval, the following equation applies, (23) – (29).

$$V_{lk1} = V_{in} - V_m \tag{23}$$

$$V_{lk2} = V_{in} - V_{out} + V_m \tag{24}$$

$$d = 1 - D \tag{25}$$

$$V_m = \frac{L_m}{L_{lk} + 2L_m} V_{out} \tag{26}$$

$$\Delta I_{L1\_II} = \frac{V_{out}}{L_{lk}}\left(1 - D - \frac{L_m}{L_{lk} + 2L_m}\right)(1-D)T_S \tag{27}$$

$$\Delta I_{L2\_II} = \frac{V_{out}}{L_{lk}}\left(\frac{L_m}{L_{lk} + 2L_m} - D\right)(1-D)T_S \tag{28}$$

$$\Delta I_{in} = \Delta I_{L1\_II} + \Delta I_{L2\_II} = \frac{V_{out}}{L_{lk}}(1-2D)(1-D)T_S \tag{29}$$

From (3), (11) and (16) is evident that input current ripple is the same (except the negative sign in (16)) under the condition that leakage inductance L_{lk} is equaled to non-coupled inductance L. If we substitute the value of duty ratio into the equations (22) and (28) we find that the ripple is same as in the equation (3), (11) and (16). The condition of D < 0.5 for equation (22) and D > 0.5 for equation (28) must be fulfilled.

The coupling coefficient k is the most important parameter which affects inductor current ripple, (30).

$$k = \frac{L_m}{L_{lk} + L_m} \tag{30}$$

Using the high value of the coupling coefficient (near 1) then the leakage inductance is almost zero. It leads to increasing of the input current ripple ΔI_{in}, but the ripple of the phase current ΔI_{L1} or ΔI_{L2} is minimized. Using the smaller value, the magnetizing inductance is smaller and the ripple of the phase current is higher. But, the ripple of the input current is smaller because of higher leakage inductance. Then, the bulky input filter is reduced. Therefore, there is a trade-off between choosing coupling coefficient.

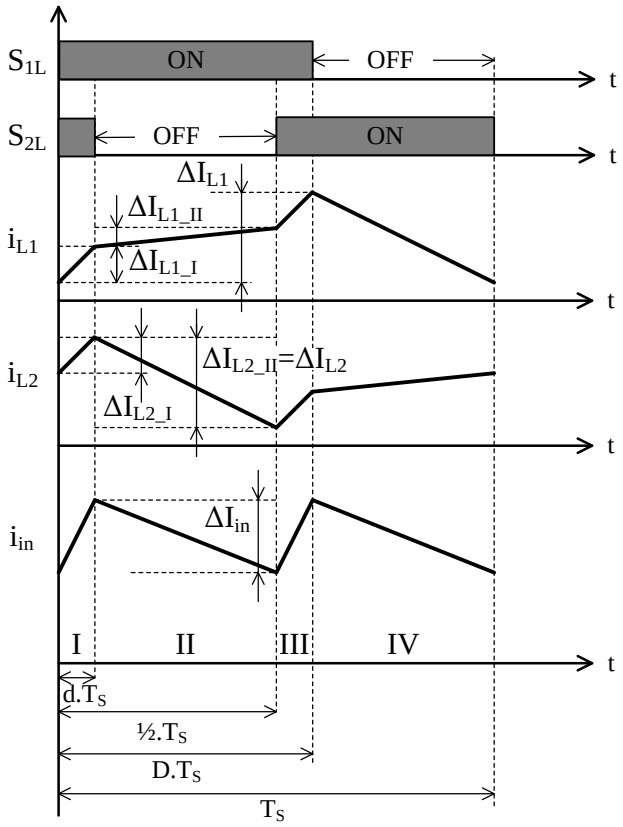

Fig. 6:Current ripples of interleaved coupled buck converter for D > 0.5

III. Simulation Results

As mentioned in section II, the inductor current ripple is strongly dependent on the coupling coefficient k of the coupled inductor. In order to have the maximum inductor current ripple reduction, the coupled inductor should have high k and also have enough leakage inductance to maintain input current ripple respectively.

The switching frequency of the one leg of the interleaved converter was set to 20 kHz, due to use of the inverter. Therefore, because of the interleaving effect, the switching frequency (input ripple frequency) is doubled, which is shown in Fig. 7, Fig.8 and Fig. 9. The self-inductance of the non-coupled inductor was set at 370 µH. In order to satisfy the condition of the ripple current equality, the leakage inductance was also set to 370 µH. Then, the coupling coefficient of the proposed coupled inductor has a value of 0.68 and it follows that the magnetizing inductance is 784 µH. The additional parameters of the converter are given in a Tab. 1. The simulation results are done for duty ratio 34% (maximum input voltage), 50% (almost zero current input ripple) and 60% (minimum input voltage).

Table 1 Setup condition

Parameters	**Coupled Inductor**	**Non-Coupled Inductor**
Switching frequency	20 kHz	20 kHz
Leakage inductance	370 µH	-
Magnetizing inductance	784 µH	-
Self-inductance	-	370 µH
Duty cycle	0.34 – 0.6	0.34 -0.6
Input voltage	150 – 250 V	150 – 250 V
Output voltage	390 V	390 V

The time waveforms of ripple current for the maximum and minimum value of duty cycle is depicted in Fig. 7 and Fig. 8. From the simulation results in Fig. 7 and Fig. 8 is evident that the inductor current ripple of the converter with a coupled inductor (i_{L3}, i_L4) is smaller than the non-coupled case (i_{L1}, i_{L2}). In Fig. 9 are given time waveforms of ripple currents for non-coupled (i_L1, i_{L2}) coupled inductor (i_{L3}, i_{L4}) with the difference that the ripple of input current (Δi_{V1} and Δi_{V2}) equals almost zero. The advantage is not in zero value of input current because same option occurs in interleaved connection with a non-coupled inductor (50%), but the fact that there is reduced inductor current ripple.

The comparison of the ratio between input and inductor current is depicted in Fig. 10. It is obvious, that the ratio is increased when the coupling effect is utilized. This means that the inductor current ripple is smaller in a whole range of duty cycle, instead of D = 0.5 (ripple is equal). To satisfy the same ripple of the input current for the coupled and non-coupled case the condition of the same leakage inductance must agree. That means the leakage inductance is same as the self-inductance in non-coupled case.

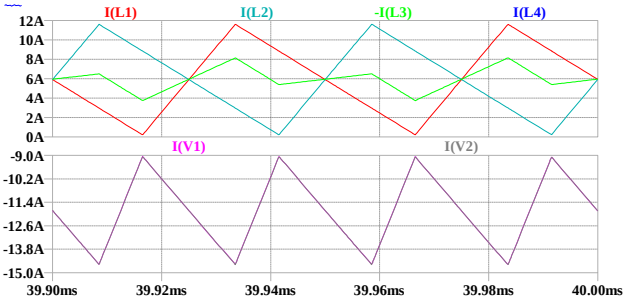

Fig. 7:Inductor current ripples with D = 34% for coupled (I(L3) and I(L4|) and non-coupled inductor (I(L1) and I(L2))-up, input current ripples for coupled (I(V1)) and non-coupled inductor(I(V2))-down

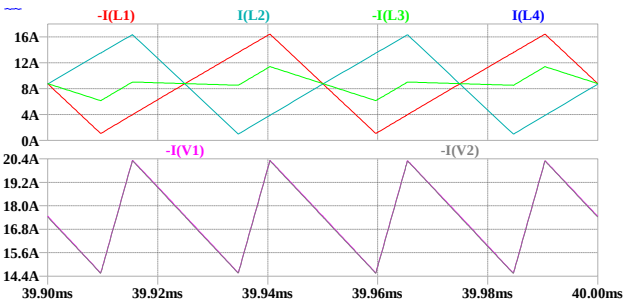

Fig. 8:Inductor current ripples with D = 60% for coupled (I(L3) and I(L4|) and non-coupled inductor (I(L1) and I(L2))-up, input current ripples for coupled (I(V1)) and non-coupled inductor(I(V2))-down

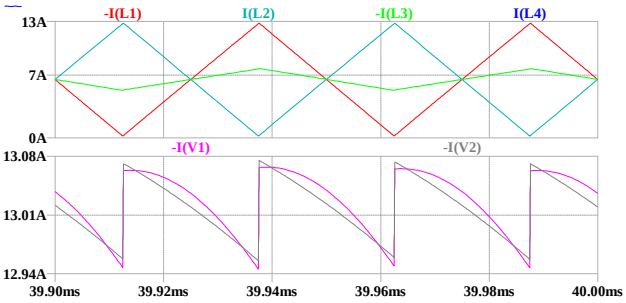

Fig. 9:Inductor current ripples with D = 50% for coupled (I(L3) and I(L4|) and non-coupled inductor (I(L1) and I(L2))-up, input current ripples for coupled (I(V1)) and non-coupled inductor(I(V2))-down

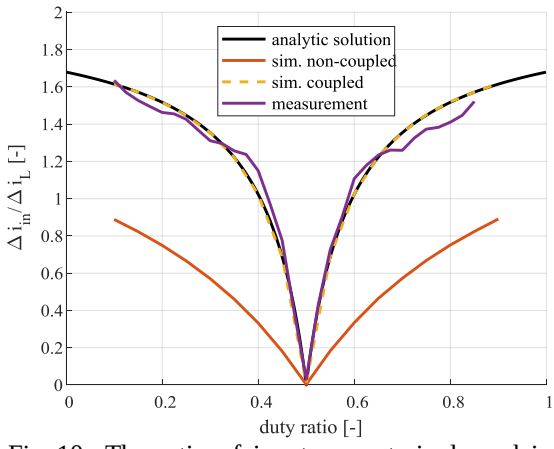

Fig. 10: The ratio of input current ripple and inductor current ripple for analytic solution (coupled), simulation (non- and coupled) and measurement (coupled)

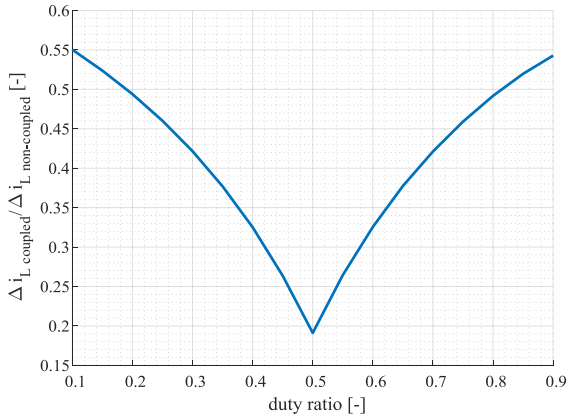

Fig. 11: The ratio of coupled inductor current ripple to non-coupled inductor current ripple

In contrast with Fig. 10, in Fig. 11 it is seen that there is a ratio of inductor currents and the ripple of the coupled inductor current is smaller than the non-coupled case in the whole range of duty cycle.

IV. Experimental Verification

In coupled inductor design, there should be a problem how to maintain the required leakage inductance. The easiest way how to manage this issue, it is used the additional non-coupled inductor. The powder core is ideal for this inductor, which is capable to carry high dc current. Then the magnetizing inductance will wound as a coupled inductor and only the ac component of the current will flow through it because the dc current is canceled with the negative coupling of the inductors. It means, that the inductors are wound against each other and the magnetic flux of both inductors is canceled. Therefore, the solution with the ferrite core should be utilized. The proposed coupled inductor in this paper does not use an additional inductor. The coils consist of two EE cores, where each winding is wound on the outer leg of the core. This ensures a sufficiently large value of leakage inductor and magnetizing inductance is adjusted with a change of an air gap in the center leg or the outer legs.

The final values of the leakage and magnetizing inductance are given in Tab. 1.

Subsequently, the experimental measurements of the converter with a coupled inductor were performed.

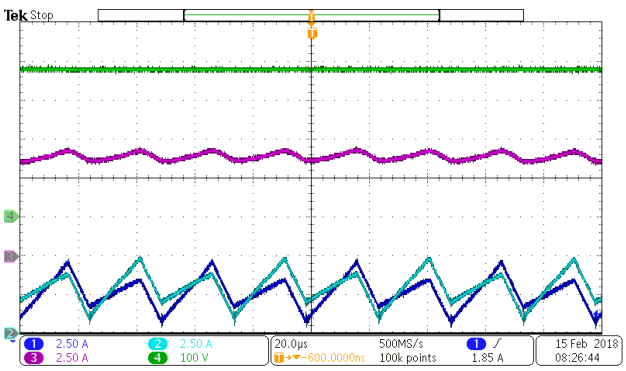

Fig. 12: The time waveforms of inductor current ripple (turquoise and blue one), input current (violet) and input voltage (green) for D < 0.5, D = 0.34

The oscilloscope waveform with the duty lower than 50% (minimum operating duty ratio – 34%) is shown in Fig. 12 and for duty higher than 50% (maximum operating duty ratio – 60%) in a Fig. 13.

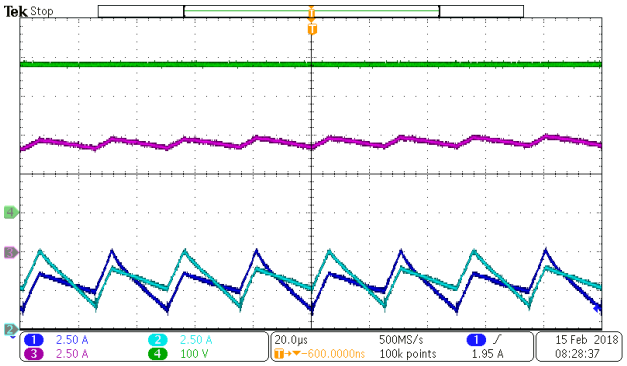

Fig. 13: The time waveforms of inductor current ripple (turquoise and blue one), input current (violet) and input voltage (green) for D > 0.5, D = 0.6

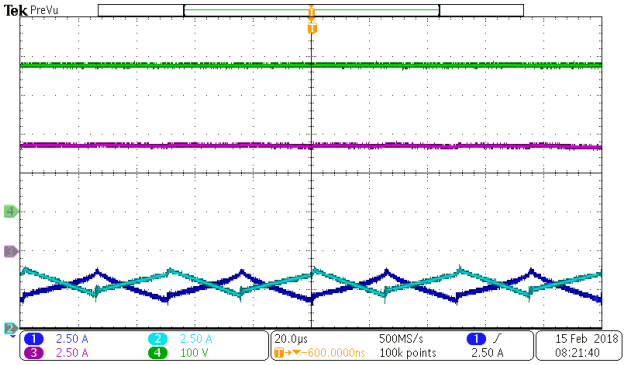

Fig. 14: The time waveforms of inductor current ripple (turquoise and blue one), input current (violet) and input voltage (green) for D = 0.5

In Fig. 12 and Fig. 13 is shown the waveform of the input and inductor currents with the minimum and maximum operating point of the converter. From Fig. 14, is visible that the ripple of the input current is markedly reduced which allows to use smaller input capacitor value and extend the lifetime of the ultracapacitor/battery pack connected to the input of the converter.

V. Conclusion

In order to reduce inductor current ripple as well as input current ripple respectively, the two inductors should be coupled to the same core. It is preferable to use coupled inductor topology in battery/ultracapacitor application due to less stress of these energy sources and lower conduction losses of the semiconductor switches because of the lower effective value of the inductor current ripple. To maintain the required ripples on the inductor and on the input respectively, the coupling coefficient must agree. For the output current, the leakage inductance is very important and it must be equal to the non-coupled inductance to maintain criterion. Then, for the high value of coupling coefficient, the mutual inductance increases and leakage inductance decreases and vice versa. The solution is to find an appropriate compromise between the output and inductor ripple value.

In the future work, the three and four phase converters with a coupled inductor will be investigated.

ACKNOWLEDGMENT

This paper is supported by the following project: APVV-15-0571.

REFERENCES

[1] S.J. KIM, H.L. DO. Interleaved Flyback Converter with a Lossless Snubber. *International Review of Electrical Engineering (IREE)*, vol. 9, iss. 5, 2014, pp. 882 – 888. ISSN 1827-6660.

[2] T. AZIB, M. BENDALI, Ch. LAROUCI and K. E. HEMSAS. Fault Tolerant Control of Interleaved Buck Converter for Automotive *Application. International Review of Electrical Engineering (IREE)*, vol. 10, iss. 3, 2015, pp. 336 – 343. ISSN 1827-6660.

[3] K.C. Tseng, J.Z. Chen, J.T. Lin, C.C. Huang, T.H. Yen, High Step-up Interleaved Forward-Flyback Boost Converter with Three-Winding Coupled Inductors. *IEEE Trans. Power Electron*. 2015, 30, 4696–4703.

[4] X .Huang, F.C. Lee, Q. Li, W. Du, W. High-Frequency High-Efficiency GaN-Based Interleaved CRM Bidirectional Buck/Boost Converter with Inverse Coupled Inductor. *IEEE Trans. Power Electron*. 2016, 31, 4343–4352.

[5] X. Hu, G. Dai, L. Wang, C. Gong, A Three-State Switching Boost Converter MixedWith Magnetic Coupling and Voltage Multiplier Techniques for High Gain Conversion. *IEEE Trans. Power Electron*. 2016, 31, 2991–3001.

[6] H. Liu, D. Zhang, Two-Phase Interleaved Inverse-Coupled Inductor Boost without Right Half-Plane Zeros. *IEEE Trans. Power Electron*. 2017, 32, 1844–1859.

[7] Y.-T.Chen, Z.-X. Lu, R.-H. Liang, Analysis and Design of a Novel High-Step-Up DC/DC Converter with Coupled Inductors. *IEEE Trans. Power Electron*. 2018, 33, 425–436.

[8] J.P. LEE, H. CHA, D. SHIN K.J. LEE. Analysis and Design of Coupled Inductors for Two-Phase Interleaved DC-DC Converters. *Journal of Power Electronics*, vol. 13, iss. 3, pp. 339-348, ISSN 1598-2092.

[9] M. Zivanov, B. Sasic, M. Lazic, . Desing of Multiphase Boost Converter for Hybrid Fuel Cell/Battery Power Sources. *In Paths to Sustainable Energy*, InTech Rijeka, Croatia, 2010; pp. 359–404, ISBN 978-953-307-401-6.

[10] J. PERDULAK, D. KOVAC, I. KOVACOVA, M. OCILKA, A. GLADYR, D. MAMCHUR, I. ZACHEPA, T. VINCE, J. MOLNAR. Effective utilization of photovoltaic energy using multiphase boost converter in compare with single phase boost converter. *CSL Communications – Scientific letters of university of Zilina*, vol. 15, iss.3, 2013, ISSN 1335-4205.

[11] D. Ebisumoto, M. Ishihara, S. Kimura, W. Martinez, M. Noah, M. Yamamoto, J. Imaoka, Design of a four-phase interleaved boost circuit with closed-coupled inductors. *Proceedings of the IEEE Energy Conversion Congress and Exposition (ECCE)*, Milwaukee, WI, USA, 2016.

[12] M. Frivaldsky, B. Hanko, M. Prazenica, J. Morgos, High Gain Boost Interleaved Converters with Coupled Inductors and with Demagnetizing Circuits, *Energies*, 2018, 11, 130.

[13] H. Kosai, S. McNeal, A. Page, B. Jordan, J. Scofield, B. Ray, Characterizing the Effects of Inductor Coupling on the Performance of an Interleaved Boost Converter. *IEEE Trans. Mag*. 2009, 45, 4812–4815.

[14] T. BERES, M. OLEJAR J. DUDRIK. Bi-directional DC/DC converter for hybrid battery.In: *14th International Power Electronics and Motion Control Conference (EPE/PEMC)*, Ohrid (Macedonia): IEEE, 2010, pp.T9-78,T9-81, ISBN 978-1-4244-7856-9.

[15] K. KROICS, U. SIRMELIS and V. BRAZIS. Design of coupled inductor for interleaved boost converter. *Przeglad Elektrotechniczny*, vol. 90, iss. 12, pp. 91 – 94, 2014, ISSN 0033-2097.

[16] P. SPANIK, M. FRIVALDSKY, P. DRGONA, J. KUCHTA. Properties of SiC Power Diodes and their Performance Investigation in CCM PFC Boost Converter. *17th International Conference on Electrical Drives and Power Electronics EDPE 2013*, 6th joint Croatian-Slovak Conference, October 2–4, 2013, Dubrovnik (Croatia), pp. 22-25, ISBN 978-953-56937-8-9, ISSN 1339-3944.

[17] J. DUDRIK, P. SPANIK, N. D. TRIP, Zero-Voltage and Zero-Current Switching Full-Bridge; DC Converter With Auxiliary Transformer, *IEEE Transactions on Power Electronics*, vol. 21, iss. 5, pp. 1328 - 1335, ISSN 0885- 8993.

[18] G. ESFANDIARI, H. ARAN, M. EBRAHIMI. Comprehensive Design of a 100 kW/400 V High Performance AC-DC Converter. *Advances in Electrical and Electronic Engineering*, 2015, vol. 13, iss. 5, pp. 417 – 429, ISSN 1336-1376.

Slavomir Kascak was born in Krompachy, Slovakia. He received the M.Sc. degree in power electronics and the D.Sc. degree in automation focused on electrical drives from the Faculty of Electrical Engineering of the University of Zilina, Slovakia, in 2010 and 2013, respectively. He is currently a Researcher and an Assistant Professor in Department of Mechatronics and Electronics. His current research activities include power electronics, electrical drives, and control.

Michal Prazenica was born in 1985 in Zilina (Slovakia). He is graduated from the University of Žilina (2009). He received the Ph.D. degree in Power Electronics from the same university in 2012. He is now Research worker at the Department of Mechatronics and Electronics at the Faculty of Electrical Engineering, University of Zilina. His research interest includes analysis and modeling of power electronic systems, electrical machines, electric drives, and control.

Miriam Jarabicova was born in Zilina, Slovakia. She received the M. Sc. Degree in Telecommunication focused on telecommunication technics from the Faculty of Electrical Engineering of the University of Zilina, Slovakia in 1999. From 1999 to 2016 she was with Elteco company as a layout engineer specialist. She is currently an internal Ph.D. student at the University of Zilina - Department of Mechatronics and Electronics in the power electrical engineering study program. The main research interest is about power electronic systems.